Statistical optimization of waste molasses-based exopolysaccharides and self-sustainable bioelectricity production for dual chamber microbial fuel cell by *Bacillus piscis*

Ebtehag A. E. Sakr[1*], Dena Z. Khater[2], Zeinab M. H. Kheiralla[1] and Kamel M. El-khatib[2]

Abstract

Background The application of exopolysaccharide-producing bacteria (EPS) in dual chamber microbial fuel cells (DCMFC) is critical which can minimize the chemical oxygen demand (COD) of molasses with bioelectricity production. Hence, our study aimed to evaluate the EPS production by the novel strain *Bacillus piscis* by using molasses waste. Therefore, statistical modeling was used to optimize the EPS production. Its structure was characterized by UV, FTIR, NMR, and monosaccharides compositions. Eventually, to highlight *B. piscis'* adaptability in energy applications, bioelectricity production by this organism was studied in the BCMFC fed by an optimized molasses medium.

Results *B. piscis* OK324045 characterized by 16S rRNA is a potent EPS-forming organism and yielded a 6.42-fold increase upon supplementation of molasses (5%), $MgSO_4$ (0.05%), and inoculum size (4%). The novel exopolysaccharide produced by *Bacillus* sp. (EPS-BP5M) was confirmed by the structural analysis. The findings indicated that the MFC's maximum close circuit voltage (CCV) was 265 mV. The strain enhanced the performance of DCMFC achieving maximum power density (PD) of 31.98 mW m^{-2}, COD removal rate of 90.91%, and color removal of 27.68%. Furthermore, cyclic voltammetry (CV) revealed that anodic biofilms may directly transfer electrons to anodes without the use of external redox mediators. Additionally, CV measurements made at various sweep scan rates to evaluate the kinetic studies showed that the electron charge transfer was irreversible. The SEM images showed the biofilm growth distributed over the electrode's surface.

Conclusions This study offers a novel *B. piscis* strain for EPS-BP5M production, COD removal, decolorization, and electricity generation of the optimized molasses medium in MFCs. The biosynthesis of EPS-BP5M by a *Bacillus piscis* strain and its electrochemical activity has never been documented before. The approach adopted will provide significant benefits to sugar industries by generating bioelectricity using molasses as fuel and providing a viable way to improve molasses wastewater treatment.

Keywords *Bacillus piscis*, Optimized molasses-based media, EPS, COD removal, Decolorization, Electrochemical activity

*Correspondence:
Ebtehag A. E. Sakr
Ebtehag.Abdelfattah@women.asu.edu.eg; ebtehagsakr@yahoo.com
Full list of author information is available at the end of the article

Sakr *et al. Microbial Cell Factories* (2023) 22:202

Page 2 of 20

Introduction

The most serious issue now plaguing the globe is thought to be climate change. The global depletion of fossil fuels and its detrimental effects on the environment might be seen as the fundamental obstacle to resolving the environmental health issue. Therefore, the search for environmentally friendly technology is viewed as the most promising method of producing sustainable energy [1, 2]. Among renewable energy sources like wind and solar energy, microbial fuel cells (MFCs) are regarded as a new sewage treatment method [3]. MFCs are employed to oxidize different organic substrates through bacterial metabolism in order to produce bioelectricity and eliminate pollutants at the same time [4, 5]. MFCs typically come in one of two designs: a single chamber or two chambers divided by a proton exchange membrane (PEM). The spotlight here is a dual-chamber MFC [6], as illustrated in Fig. 1.

The dual-chamber MFCs are appropriate for anaerobic digestion, bioelectricity generation, wastewater treatment, low energy consumption, low running costs, low sludge production, and clean techniques [7]. Currently, the main factors impeding its advancement are poor power output, high cost, and inadequate wastewater treatment [7]. Electricigens, the MFC's structure, the characteristics of the substrate, external and internal resistances, and the materials used for the electrodes are the foremost issues that have an impact on performance. Simple molecules including sucrose, glucose, fructose, ethanol, and acetate, as well as various wastewater from domestic, industrial, and agricultural sources, can be used as substrates [8]. Several investigations have been done in the past using easily degradable sugars added exogenously to the MFC to generate electricity. However, the performance of the process varies in real-world applications using wastewater depending on the wastes utilized as the substrates and the microorganisms present [9, 10].

Molasses is a syrupy by-product of the sugarcane industry and has a thick, viscous, and dark brown color [11]. Its use as a raw material for the generation of bio-fuels such as bioethanol, biodiesel, biogas, hydrogen, and methane as well as bio-electricity results in significant amounts of molasses wastewater [12]. Before discharging it into the environment, a suitable wastewater treatment system is needed because dumping it into the water system could result in major pollution, including foul odor and taste as well as effects on the city's water supply and aquatic inhabitants [13]. Some techniques, including anaerobic treatment, adsorption, flocculation precipitation, catalytic oxidation, and membrane separation, are the primary ways for treating molasses wastewater. These techniques share the traits of being expensive and producing harmful byproducts. It is important to look at more suitable treatment options as we deal with the simultaneous challenges of energy shortages and environmental pollution. Due to its poor fluidity, high concentration of organic acids, high color, low pH, and significant corrosivity, molasses has not received much research, however some findings from earlier years have shown that it is an effective electron donor in MFCs [4, 8].

Molasses wastewater contains between 40 and 55% sucrose and has a pH between 5.5 and 6.5. It can be used as a cheap substrate for MFCs because it contains the majority of the nutrients, such as sugar, protein, amino acids, and vitamins, which improve the production of biomass and EPS when used by microbes for the reduction of most molasses into small molecular sugars that are easier for microorganisms to use [14]. According to the literature, total COD removal efficiencies attained with MFC systems have ranged from 45.7 to 90.3%, and the maximum power density (MPD) has been reported to have ranged from 8.8 to 1410.2 mW m^{-2} [15, 16]. For instance, a stacking MFC was created to handle molasses wastewater, and its MPD was 115.5 mW m^{-2} [17].

Microbes linked to MFC produce a thin layer of microbial growth called biofilm that adheres to the electrodes [18]. The location where the biofilm develops controls the bacteria's ability to produce electrons and has a substantial impact on the disintegration of various organic materials in MFC [18]. For the development of biofilms, EPS and lipopolysaccharides are essential. Recent studies have shown evidence that the EPS in electroactive biofilm (EAB), which connects cells to cells over the electrode, is electrically conductive [19]. The synthesis of EPS is often regarded as one of the strategies employed by microorganisms to endure environmental stress [20]. Therefore, EPS producing bacteria was isolated from molasses.
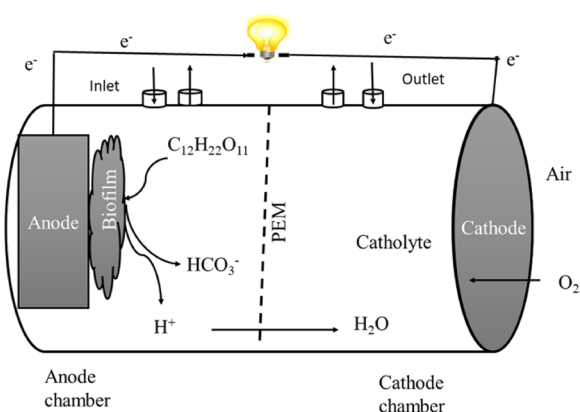
Fig. 1 A conceptual view of a dual-chamber MFC experimental system

Sakr *et al. Microbial Cell Factories* (2023) 22:202

Page 3 of 20

Bacillus sp. has been proven to be a potent source of EPS production [21] and produces more varieties and larger amounts of EPS [22]. Rarely is molasses employed in the production of polysaccharides [23]. Meanwhile, some polysaccharides such as pullulan, welan gum, and glucan have all been produced from molasses [24–26]. For improved EPS production with the development of a less expensive medium, the growth parameters were optimized using Plackett–Burman design (PBD) and statistical design response surface methods (RSM). RSM is one of the effective statistical methods for planning experiments, developing models, identifying the best combinations of variables to produce desired results, and assessing the relative importance of various influencing factors even in the face of complex interactions [27]. One of the most widely utilized experimental models in the RSM for maximizing the production of EPS from *Bacillus licheniformis* NS032 in a medium based on sugar beet molasses is the Box-Behnken Design (BBD) [28]. With this approach, a large number of factors can be optimized simultaneously, and a small number of experimental runs can yield a lot of large quantitative information [29]. An exciting area of research for industrial biotechnologists is the optimization and characterization of innovative EPS-BP5M synthesis from *Bacillus* sp. grown on inexpensive molasses using an ecologically friendly microbial method. It is important to note that the research on EPS-BP5M and bioelectricity production from molasses optimization via this strain has not yet been reported elsewhere.

This study was designed to screen the bacterial isolates from molasses for their ability to synthesize EPS-BP5M and identify the best candidate for bio-based polymer production. The EPS-BP5M yield was optimized by PBD and RSM for the highest EPS-producing bacteria. Then, the structural characterization of EPS-BP5M was done by Fourier-transform infrared (FTIR) analysis, proton nuclear magnetic resonance (^{1}H-NMR), elemental analysis, and High-Performance Liquid Chromatography (HPLC). Also, the present study was focused on exploring the EPS producing *Bacillus* sp. for DCMFC electricity production using optimized molasses as a growth medium. Various parameters like OCV, CCV, current density, polarization curve, CE, CV, and its kinetic studies, and anodic biofilm were analyzed by SEM. The removals of COD and color presented in the molasses media were monitored.

Results

Chemical analysis of sugarcane molasses
The amount of sugar was found to be fermentable (39.98%) and un-fermentable (4.30%). 48.76% of the total sugar can be regarded as a potential carbon source for many microorganisms. The amounts of residual sugar,

inverted sugar, ash content, and pH were 4.21%, 18.60%, 13.10%, and 5.6, respectively (Table 1).

Isolation, selection, and genotypic identification of the potent EPS producing isolate
Five colonies (1-Mol–5-Mol) isolated from molasses were chosen in light of the observation of mucous growth surrounding its colonies on agar plates. The isolate 5-Mol was determined to have the largest EPS production (5.78 g L^{-1} of medium) than the other isolates, making it a promising candidate for EPS production.

The 5-Mol isolate was identified molecularly utilizing the partially sequenced 16S rRNA genes and revealed to be a member of the genus *Bacillus* with a 99.88% identity to the species *B. piscis* with a query cover of 100%. A phylogenetic tree (Fig. 2) based on 16S rRNA gene sequences was created to show the relative positions of this strain (5-Mol) and other *Bacillus* species. The sequence was additionally submitted into the GenBank database (NCBI) under accession number OK324045. The identified strain was designated as *B. piscis* strain 5-mol. *B. piscis* has never before been isolated from molasses.
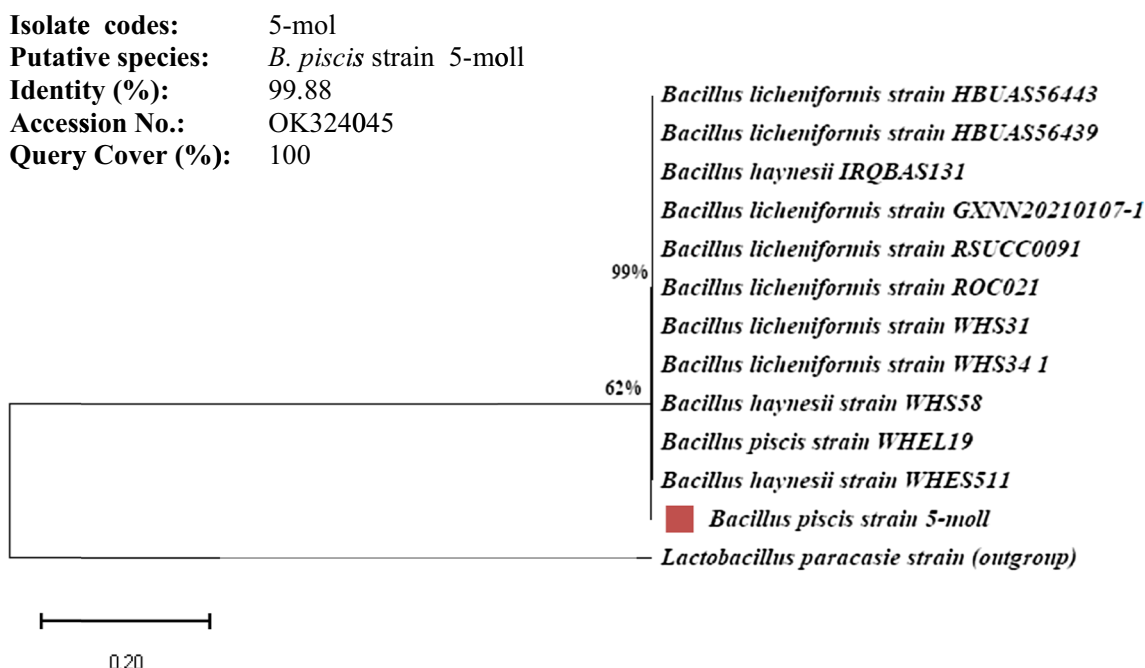
Statistical optimization of molasses based-medium for EPS-BP5M production by B. piscis
Plackett–Burman design (PBD)
Utilizing a cheap nutrient source like sugarcane molasses (industrial waste) is one of the cost-effective solutions for the growth of *B. piscis.* In this study, the PBD was used in 12 runs to screen a total of 11 factors for their impact on the EPS-BP5M synthesis (Table 2). Bacterial EPS-BP5M varied significantly from 12.12 to 27.50 g L^{-1}. This

Table 1 The physicochemical parameters and EPS yield of bacterial isolates of sugarcane molasses

	Values
Physicochemical parameters	
pH	5.60
Total sugar (TS), %	48.76
Total Fermentable sugars (TFS), %	39.98
Non-fermentable sugars (NFS), %	4.30
Residual sugar (RS), %	4.21
Inverted sugar, %	18.60
Ash	13.10
Brix	83.93
EPS yield (g/L) of bacterial molasses isolates	
1-Mol	2.94
2-Mol	2.90
3-Mol	2.46
4-Mol	1.26
5-Mol	5.78

Sakr *et al. Microbial Cell Factories* (2023) 22:202

Page 4 of 20

Isolate codes: 5-mol
Putative species: *B. piscis* strain 5-moll
Identity (%): 99.88
Accession No.: OK324045
Query Cover (%): 100

Fig. 2 Phylogenetic relationships between 5-mol isolate and 16S rRNA gene sequences retrieved from the GenBank database

variation demonstrated the importance of optimization for achieving the highest yield of EPS-BP5M. The greatest EPS-BP5M yield (27.5 g L^{-1}) was recorded in run No. 1, whereas run No. 4 showed the lowest EPS-BP5M production (12.12 g L^{-1}, Table 2).

The first-order polynomial (Eq. 1), which depicts the association between each variable and the EPS-BP5M yield, was constructed from the PBD data as follows:

$$
\begin{aligned}
&Yield\ of\ EPS{-}BP5M\ \left(gL^{-1}\right)\\
&= 13.52569 + 1.6575 * Sugarcane\ molasses,\ (X1)\\
&\quad + 0.61583 * Yeast\ extract,\ (X2)\\
&\quad - 3.19667 * NaCl,\ (X4)\\
&\quad + 3.83611 * MgSO_4,\ (X8)\\
&\quad - 0.8675 * MgCl,\ (X9)\\
&\quad + 0.64042 * Inoculum\ size,\ (X10)\\
&\quad - 0.70417 * pH,\ (X11)
\end{aligned}
\tag{1}
$$

Molasses, $MgSO_4$, MgCl, and inoculum size were shown to significantly affect the production of EPS-BP5M with P-values below the significance level in the statistical analysis using PBD (Table 3), while the remaining components were determined to be insignificant with P-values above 0.05 for all of them. F-test was used to determine the significance of the fitting equation. The model was extremely significant ($p = 0.0009 < 0.01$) and

the R^2 was 0.9013 and the adjusted R^2 was 0.9698, which indicated a good model fit.

A Pareto chart (Fig. 3) illustrates how the t-value and rankings are related. Depending on the significance level, the Pareto chart indicates the significance and magnitude of the factors that affect the EPS-BP5M production. Effects that exceed the t-value upper limit 2.776 are considered significant. The three variables [molasses (A), $MgSO_4$ (K), and inoculum size (H)] were discovered to have a substantial impact on the intended response of EPS-BP5M production based on the effects and P-values (Table 3).

Box–Behnken design (BBD)

The BBD of RSM was used to ascertain the ideal levels of the three chosen variables (molasses, $MgSO_4$, and inoculum size) based on the PBD analysis. Table 4 presents the design matrix and the associated responses. The findings of the experiment were examined using standard ANOVA. The second-order polynomial equation (Eq. 2) was used to fit the BBD:

$$
\begin{aligned}
Y\ (g\,L^{-1}) =&\ 106.66 + 12.90X1\\
&+ 201.38X2 + 27.37X3\\
&+ 0.28X1X2 + 8.75E\\
&- 03X1X3 - 1.14X2X3\\
&- 1.13X1^2 - 196.61X2^2 - 3.26X3^2
\end{aligned}
\tag{2}
$$

Table 2 Optimization of EPS-BP5M production from *B. piscis* in molasses-based medium by PBD

Run	F1 A: Molasses, (X1)	F2 B: Yeast ex., (X2)	F3 C: Peptone ex., (X3)	F4 D: NaCl, (X4)	F5 E: KH$_2$PO4, (X5)	F6 F: K$_2$HPO4, (X6)	F7 G: NaNO$_3$, (X7)	F8 H: MgSO$_4$, (X8)	F9 J: MgCl, (X9)	F10 K: Inoculum size, (X10)	F11 L: pH, (X11)	Response (EPS-BP5M Yield) Actual value	Predicted value
	%	g/L	g/L	g/L	g/L	g/L	g/L	g/L	g/L	%	pH	g/L	g/L
1	8	2	2	0.5	0.3	1	5.0	0.8	0.5	6	8	27.5	27.26
2	2	2	2	0.5	0.1	1	2.5	0.2	0.5	2	6	14.05	13.86
3	8	4	2	0.5	0.1	2	2.5	0.8	2.5	2	8	23.88	24.20
4	2	2	2	1.0	0.1	2	5.0	0.2	2.5	6	8	12.12	11.68
5	8	4	2	1.0	0.3	2	2.5	0.2	0.5	6	6	24.98	26.00
6	8	2	4	1.0	0.3	1	2.5	0.2	2.5	2	8	18.63	19.07
7	2	4	4	1.0	0.1	1	2.5	0.8	0.5	6	8	17.22	16.95
8	2	4	2	1.0	0.3	1	5.0	0.8	2.5	2	6	14.3	14.06
9	2	2	4	0.5	0.3	2	2.5	0.8	2.5	6	6	16.05	16.99
10	8	2	4	1.0	0.1	2	5.0	0.8	0.5	2	6	25.03	24.51
11	8	4	4	0.5	0.1	1	5.0	0.2	2.5	6	6	26.89	25.87
12	2	4	4	0.5	0.3	2	5.0	0.2	0.5	2	8	13.5	13.69

F factor

Sakr *et al. Microbial Cell Factories* (2023) 22:202

Page 6 of 20

Table 3 Statistical analysis of the model by PBD for EPS-BP5M yield

Source	Sum of squares	df	Mean square	F value	p value	
Model	359.48	7	51.35	51.53	0.0009*	Significant
A, (X1)	296.71	1	296.71	297.73	< 0.0001*	
B, (X2)	4.55	1	4.55	4.57	0.0994	
D, (X4)	7.66	1	7.66	7.69	0.0502	
H, (X8)	15.89	1	15.89	15.95	0.0162*	
J, (X9)	9.03	1	9.03	9.06	0.0395*	
K, (X10)	19.69	1	19.69	19.75	0.0113*	
L (X11)	5.95	1	5.95	5.97	0.0709	
Residual	3.99	4	1			
Cor total	363.47	11				
R^2	0.989					
Adj R^2	0.9698					
Pred R^2	0.9013					
Adeq. precision	19.114					

A: molasses; B: yeast ex.; D: NaCl; H: $MgSO_4$; J: MgCl; K: Inoculum size; L: pH; DF: degrees of freedom

* Significant at $P < 0.05$. The rest of other factors were non-significant
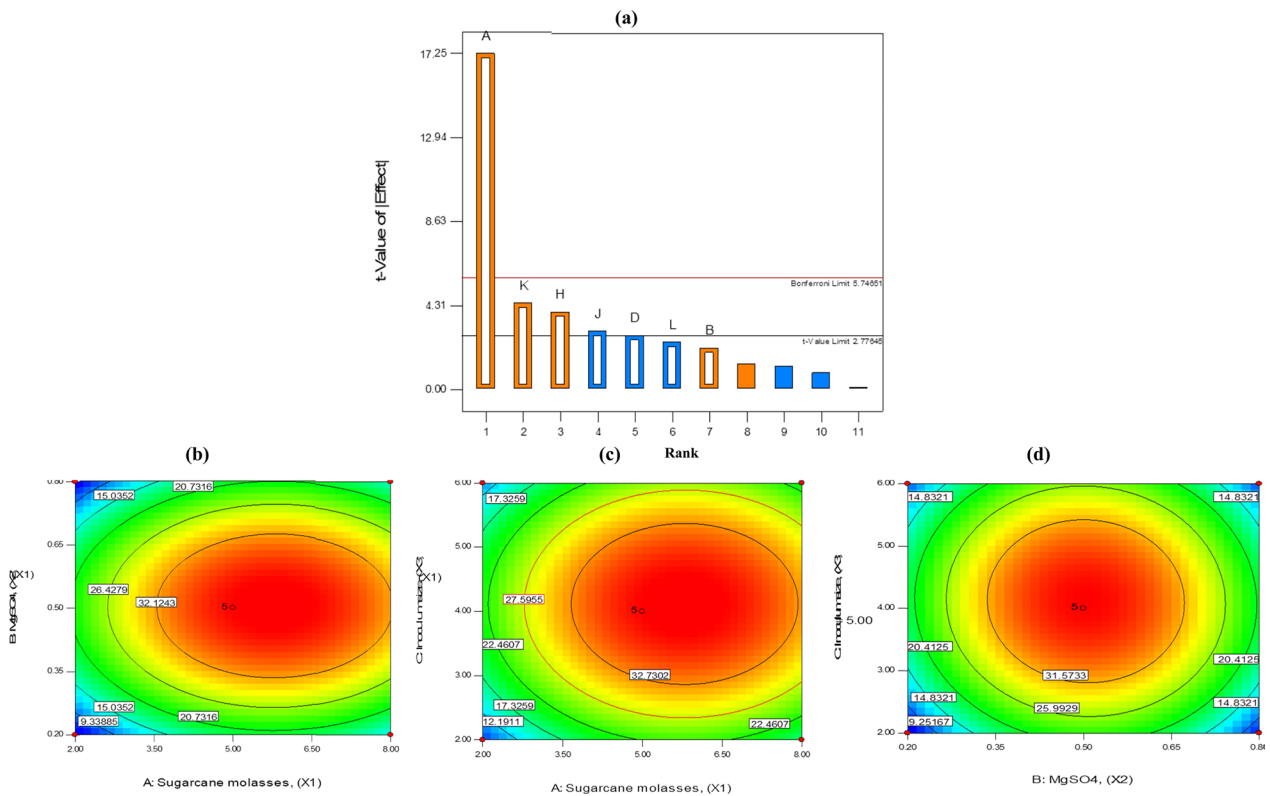
Fig. 3 Pareto diagram of the fractional factorial design used to select the variables that affect the production of EPS-BP5M (**a**). Response surface 2D counter plots showing interaction between sugar cane molasses vs. $MgSO_4$ (**b**), sugar cane molasses vs. inoculum size (**c**), and $MgSO_4$ vs. inoculum size (**d**)

Sakr *et al. Microbial Cell Factories* (2023) 22:202

Page 7 of 20

Table 4 Box–Behnken design for the production of EPS-BP5M

Run	F1 A, molasses (X1) %	F2 B, MgSO$_4$ (X2) g/L	F3 C, inoculum size (X3) %	Actual value EPS-BP5M Yield (g/L)	Predicted value
1	8	0.5	2	18.27	17.71
2	8	0.2	4	12.91	13.90
3	5	0.5	4	37.11	37.11
4	5	0.2	2	4.10	3.67
5	5	0.5	4	37.11	37.11
6	8	0.8	4	14.86	15.39
7	8	0.5	6	21.83	20.87
8	2	0.5	6	9.45	10.01
9	5	0.8	6	7.28	7.71
10	5	0.5	4	37.11	37.11
11	2	0.5	2	6.10	7.06
12	5	0.5	4	37.11	37.11
13	2	0.2	4	4.17	3.64
14	2	0.8	4	5.10	4.12
15	5	0.8	2	5.99	6.02
16	5	0.5	4	37.11	37.11
17	5	0.2	6	8.12	8.09

F factor

Table 5 ANOVA of the different responses assessed for Box-Behnken design for EPS-BP5M

Source	Sum of squares	df	Mean square	F value	p value	
Model	2993.23	9	332.58	438.11	< 0.0001[*]	Significant
A- (X1)	231.66	1	231.66	305.17	< 0.0001[*]	
B- (X2)	1.93	1	1.93	2.54	0.154	
C- (X3)	18.67	1	18.67	24.59	0.0016[*]	
AB	0.26	1	0.26	0.34	0.5767	
AC	0.011	1	0.011	0.015	0.9075	
BC	1.86	1	1.86	2.45	0.1612	
A^2	434.21	1	434.21	571.98	< 0.0001[*]	
B^2	1318.37	1	1318.37	1736.68	< 0.0001[*]	
C^2	716.24	1	716.24	943.5	< 0.0001[*]	
Residual	5.31	7	0.76			
Lack of Fit	5.31	3	1.77			
Pure Error	0	4	0			
Cor Total	2998.54	16				
R^2	0.9982					
Adj R^2	0.9959					
Pred R^2	0.9716					
Adeq. precision	50.083					

A: molasses; B: MgSO$_4$; C: Inoculum size; DF: degrees of freedom

[*] Significant at $P < 0.05$

where Y is the predicted EPS-BP5M production, X1, X2 and X3 corresponded to molasses conc., MgSO$_4$ conc., and inoculum size, respectively. The proposed model's F-value was 438.11 and its low *P*-value indicated that it is highly significant according to the statistical analysis performed using ANOVA (Table 5). The model could be used to analyze the variation in the EPS-BP5M yield because the model's R^2 value was 0.9716 and its adjusted

Sakr *et al. Microbial Cell Factories* (2023) 22:202

Page 8 of 20

R^2 value was 0.9959, demonstrating the model's fitting of the tested model and confirming the high accuracy and credibility of the test results [30]. To verify the factors' significance, "Probe > F" was utilized, which denotes how strongly independent components interact with one another. Because each "Probe > F" was less than 0.05, an ANOVA revealed that the model terms X1, X3, $X1^2$, $X2^2$, and $X3^2$ were significant.

The interactions of molasses, inoculum size, and $MgSO_4$ for the production of EPS-BP5M are depicted in a two-dimensional contour graph (Fig. 3). Because the contour plots were elliptical, significant interactions between the inoculum size and molasses and between the inoculum size and $MgSO_4$ were also seen.

The regression equation's predicted values were frequently in agreement with the experimental results, demonstrating the model's validity. According to the contour plot and regression analysis, 5% molasses, 0.5 g L^{-1} $MgSO_4$, and 4% inoculum size were the ideal conditions to obtain the highest production of EPS-BP5M. The yield was found to be 37.11 g L^{-1} under these optimized conditions with a 6.42-fold enhancement as compared to the initial production medium (5.78 g L^{-1}). These findings suggest that EPS-BP5M from *B. piscis* can be produced with a better yield during fermentation by using a waste molasses-based medium as an alternative carbon source.

Structural characterization

No absorption peaks at 260 or 280 nm were detected in the UV–Vis spectra of the EPS-BP5M (Fig. 4a), demonstrating the lack of proteins and nucleic acids [31].

FTIR spectroscopy was used to examine the chemical composition of the EPS-BP5M produced by *B. piscis* (Fig. 4b). The broad stretching peak of O–H stretching is evident at 3294 cm^{-1} [32]. At 2940 cm^{-1}, C–H stretching vibration has been found [32]. As a result of C–O stretching, the spectrum data also revealed a peak at 1656 cm^{-1} [33]. Peak between 1000 and 1110 cm^{-1}, which is indicative of the presence of α-(1 → 4) Glu*p* residue [34]. There was no peak for the β-configuration, which is expected to rise between 890 and 950 cm^{-1} [34]. The characteristic peaks of carbohydrates were a number of peaks between 1000 and 800 cm^{-1} [35]. Therefore, this molecule might facilitate biofilm formation by *B. piscis* on our MFC.

Most of the proton signals were found between 3.156 and 4.591 ppm in the ^{1}H-NMR spectrum of EPS-BP5M (Fig. 4c). Notably, two peaks (5.162 and 5.172 ppm) were found in the anomeric region, indicating the existence of
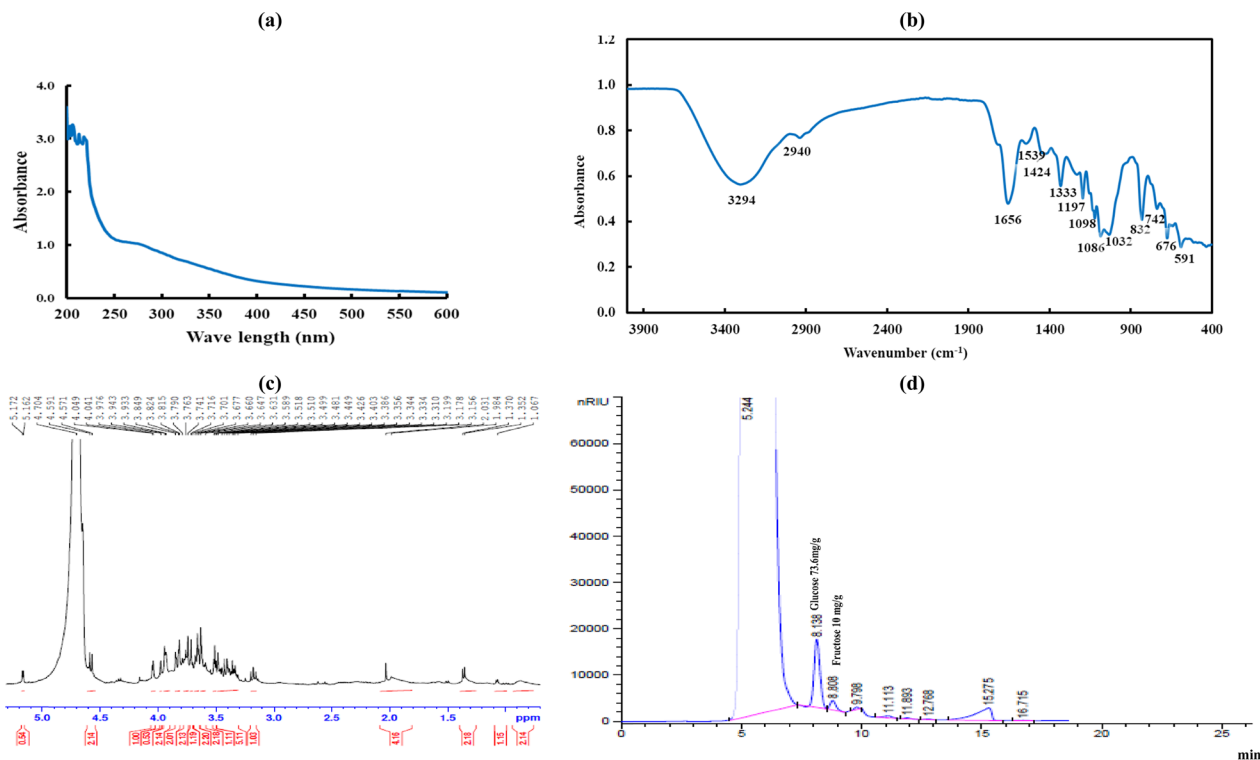
Fig. 4 UV (**a**), FTIR (**b**), NMR (**c**) spectra and monosaccharides composition (**d**) of EPS-BP5M from *B. piscis*

Sakr *et al. Microbial Cell Factories* (2023) 22:202

Page 9 of 20

Table 6 Elementary composition of the EPS-BP5M and bacterial surface properties

Parameters	Values
Elemental composition of EPS-BP5M (%)	
C	28.56
H	6.68
N	2.89
S	3.41
Bacterial surface properties	
Autoaggregation (%)	
3 h	24.12 ± 3.25
6 h	52.67 ± 1.62
24 h	73.48 ± 1.79
Hydrophobicity (%)	31.98 ± 1.12

anomeric protons. Hydrogen–deuterium oxide (HDO) is responsible for the peak at 4.70 ppm. Between 4.1 and 3.1 ppm, the frequency of HC–O (singly-oxygenated hydrogen and carbon) chemical shifts was noted [36]. This suggests that EPS-BP5M may have a higher binding capacity to the DCMFC electrode. Therefore, to establish its ability to bind to electrodes, an experiment utilizing *B. piscis* producing EPS-BP5M is required.

The findings of the elemental analysis (Table 6) revealed higher concentrations of carbon and hydrogen, indicating that the majority of the components of EPS-BP5M are sugars.

Monosaccharide analysis

The EPS-BP5M was acid hydrolyzed, and its monosaccharide composition was identified (Fig. 4d). The repeating units of this EPS-BP5M were observed by comparing the chromatographic results of the sample with the retention time of various monosaccharide standards. These repeating units were glucose (73.6 mg/g) and fructose (10.0 mg/g). This result implied that strain 5-Mol synthesized a heteropolysaccharide in an optimized molasses medium, with glucose serving as the major repeating monomer in this polysaccharide chain.

Cell surface characteristics

Bacillus sp. had hydrophobic cell surfaces and the cell autoaggregation improved over time (31.98 ± 1.12%; Table 6). The results clearly showed that EPS-BP5M alters the physicochemical characteristics of cell surfaces, indicating that hydrophobic interaction may be crucial for *B. piscis* cells' ability to adhere to carbon-felt electrode of our DCMFC.

### Utilization of optimized molasses-based medium for electricity production using *B. piscis* strain

Voltage generation

Figure 5a depicts the changes in open circuit voltages (OCVs) and close circuit voltages (CCVs) at an external resistance of 10 kΩ over time following feeding with an optimized molasses-based medium inoculated with *B. piscis*. Our strain had three phases (log, stationary, and decline phase) throughout the acclimatization period when grown on molasses over three cycles. During the log stage, each OCVs cycle started to climb linearly. Throughout 200 h, the voltage outputs gradually stabilized at maximum levels of 574, 599, and 624 mV, respectively, with very minor changes for each cycle. After the OCVs dropped to extremely low values (about 70 mV) due to the loss of fuel cell life, fresh molasses wastewater was added. In such instances, the bacterial communities in the functioning biological reactor already adjusted well to the environment of DCMFC and subsequently takes shorter periods to decrease the startup time for electricity generation [37]. Moreover, Fig. 5a illustrated the influence of 10KΩ on the performance of DCMFC outputs using molasses as an electron donor over three cycles of operation. It could be observed that the CCVs had the same previously pattern.
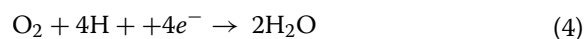
Polarization characteristics DCMFC

To ensure the accuracy of the measurement, several external loads ranging from 650 kΩ to 100 Ω were applied when the OCV reached a plateau after feeding with molasses to determine the representative steady-state polarization properties and the accompanying power density plots for DCMFC. The maximum power density (PD_{max}) was observed to be 31.98 mW m^{-2} when the current density (CD) was 185.95 mA m^{-2} and the resistance was 500 Ω at a corresponding voltage output of 172 mV (Fig. 5b). The calculated internal resistance (R_{in}) was found to be approximately 463.4 Ω. Molasses contained roughly 50% sucrose by weight, which was thought to be the primary substrate for the DCMFC. The equation for the oxidation of sucrose was determined using a stoichiometric method similar to that used for the oxidation of acetate [38].
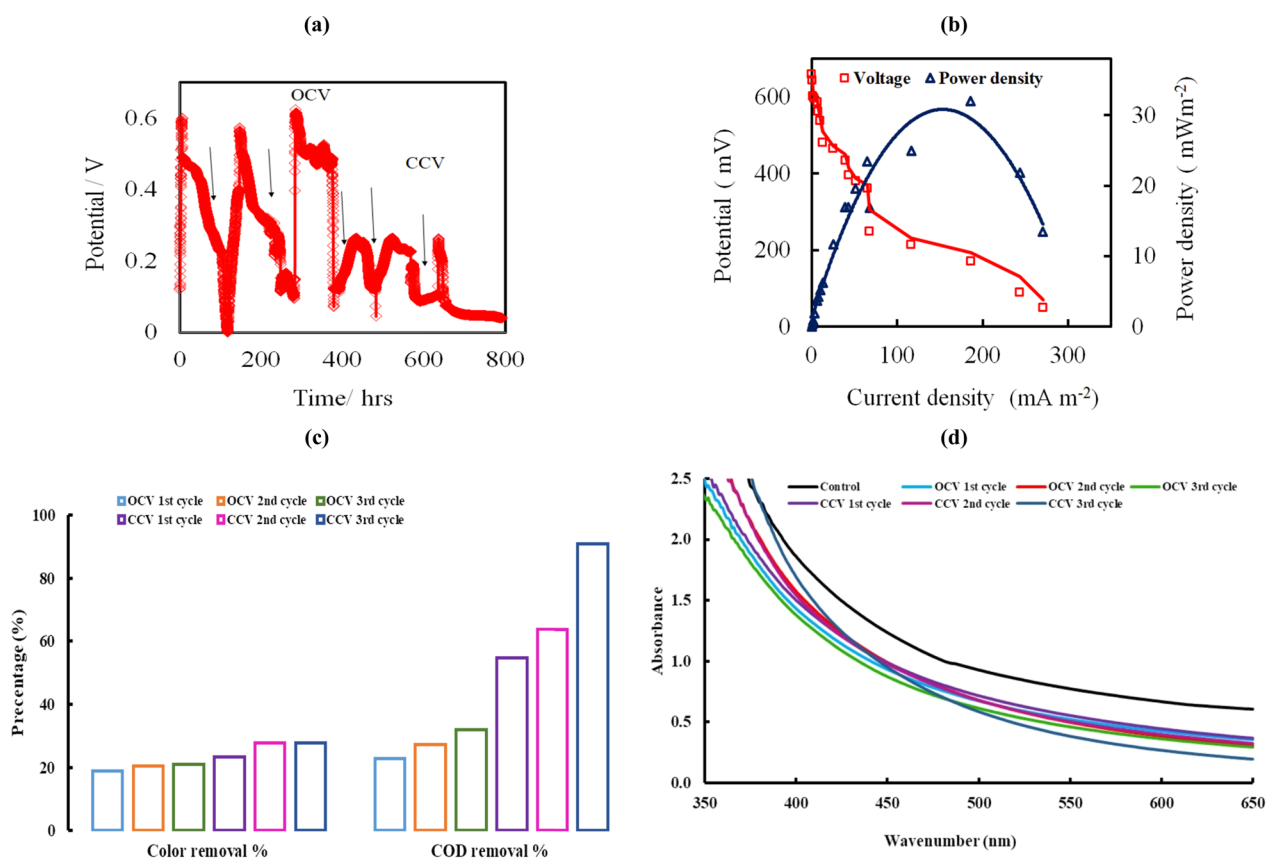
The anodic reaction is then given as follows:

$$C_{12}H_{22}O_{11} + 25H_2O \xrightarrow{B.\,piscis} 12HCO_3^- + 60H^+ + 48e^- \tag{3}$$
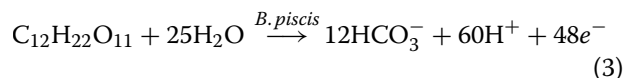
whereas, the cathodic reaction as follows:

$$O_2 + 4H + +4e^- \rightarrow 2H_2O \tag{4}$$

The polarization curve could be separated into three zones. At the high cell voltage zone, the current increased

Sakr *et al. Microbial Cell Factories* (2023) 22:202

Page 10 of 20

Fig. 5 The performance of DCMFC inoculated with *B. piscis* and molasses wastewater as anode fuel, **a** Trend of both OPVs and CCVs output values in the 800 h incubation period and **b** Power and polarization curve. **c** Color (ξcolor %) and COD removal efficiency of DCMFC after each cycle. **d** Spectral scanning (visible band) of optimized molasses media before and after MFC treatment at 37 °C, following inoculation with *B. piscis*

rapidly with the lowering of the cell voltage values, but at the intermediate voltage zone, the rate of this increase was greatly diminished. At the low cell voltage zone, the rate of the increased current became high again.

COD removal efficiency

At the end of each cycle in the DCMFC system, the variation affinity of COD and its removal rate of the molasses wastewater implemented as the anode substrate medium were assessed (Fig. 5c) at an initial COD concentration value was 22 g L^{-1}. With a removal efficiency of $25 \pm 3.2\%$, the COD averaged 16.5 g L^{-1} during the OCV cycle. While with a removal efficiency of $59 \pm 6.4\%$, the COD averaged 9 g L^{-1} during the CCV cycle. Moreover, the maximum CCV at 265 mV was obtained for 8 and 2 g L^{-1} while the minimum CCV at 10 g L^{-1} was about 262 mV. As a result, the performance was due to the breakdown of molasses by electroactive *B. piscis,* resulting in a lower COD value.

Coulombic efficiencies

The oxidation of molasses over three cycles of operations causes a flow of electrons by mature *B. piscis* biofilm at the anode chamber, which is represented by the coulombic efficiencies (CEs%). It was calculated by monitoring the variations in COD during a period following the cell's voltage reduction to less than 70 mV. The CEs were 36.94, 33.22 and 21.23% at 12, 14 g L^{-1} and 20 g L^{-1} COD, respectively. Additionally, the CE decreased as influent COD molasses concentration increased. It could be confirmed the inverse relationship between $C_E\%$ and molasses concentration.

Color removal

After DCMFC treatment, a decolorization of the molasses was observed with a decolorization of $27.68 \pm 1.52\%$ (Fig. 5c, d).

Sakr *et al. Microbial Cell Factories* (2023) 22:202

Page 11 of 20
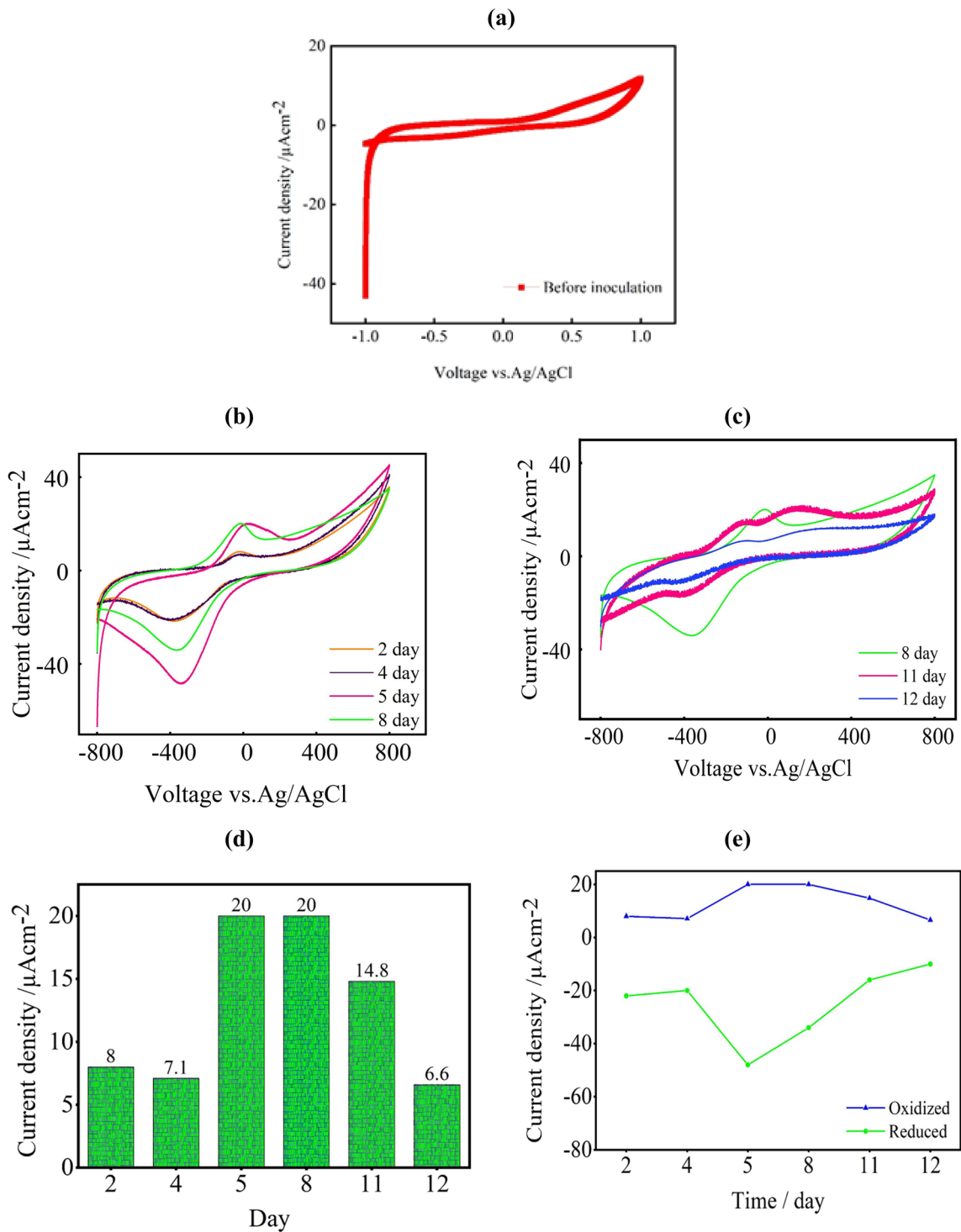
Fig. 6 The electrocatalytic activity of sterilized *B. piscis* in an anodic chamber for DCMFC using molasses as substrate, **a** CV before inoculation, **b**, **c** recorded CVs at 20 mV s^{-1} for 2, 4, 5, 8, 11, 12 days, **d** the corresponding current density in correlation with day and **e** the trend of oxidized and reduced peaks over the days

Sakr *et al. Microbial Cell Factories* (2023) 22:202

Page 12 of 20

Cyclic voltammetry (CV)

The electrocatalytic activity of *B. piscis* biomass that had been connected to the anodic electrode at various times throughout the operation was confirmed by the CV analysis. Thus, in order to determine the oxidation reduction activities and the mediators linked to the anodic chamber, a sterilized molasses media inoculated with *B. piscis* was incubated at various time intervals (0 h and 2, 4, 5, 8, 11, and 12 days) at a scan rate of 20 mV s^{-1} (Fig. 6).

The CV displayed a smooth curve prior to inoculation (0 h) with no redox peaks during the oxidation and reduction process (Fig. 6a). While the *B. piscis* displayed two reversible peaks, as shown in Fig. 6b, c, which point to the existence of redox peaks in the molasses-based media. Additionally, Fig. 6d, e depicts the trend of both oxidized and reduced peaks over the days and the produced current densities. The voltage and current of oxidized and reduced peaks were significantly shifted along the operation time, which could be related to alterations in the medium over time. Furthermore, redox peaks started to form at -24 mV after 2 days of inoculation. The oxidation and reduction peaks then started to rise at -26 mV after 4 days of incubation and ultimately reached their peak after 5 days. The highest current densities were recorded on days 5 and 8 of operation, measuring at 20.08 and 20.06 μA cm^{-2} with corresponding positive sweep potentials of 25 and 3.5 mV, respectively.

In addition, it was noted that the 11 day (-125 and -153 mV) and 12 day of operation (-140 and 210 mV) had two oxidative waves. Reduction peaks were seen in the potential range between -103 and -720 mV during the reverse scan. The released extracellular metabolites produced by *B. piscis* and the self-produced mediators that formed during the late exponential and stationary phases may be responsible for these waves [39]. After 12 days, the peak current dropped to 6.6 μA cm^{-2} at -105 mV, presumably due to nutrient depletion, as no medium refill was done [40–42]. These findings match with the cell proliferation displayed in Fig. 5a. The cell growth peaked after 5 days of operation and entered the exponential phase. These results encourage further study into whether *B. piscis* acts well as a biocatalyst for the breakdown of molasses in MFCs, taking into account the potential existence of EPS-BP5M which might accelerate the electron transfer.

CV studies at different scanning rates

On the 5th day, as shown in Fig. 7a, the CV was measured at various sweep scan rates of 5, 10, and 20 mV s^{-1} to assess the kinetic studies on the inoculated DCMFC with *B. piscis* in the anodic chamber. The increase in scan rate was accompanied by an increase in redox peaks. Additionally, the reduction peaks were modified towards a negative voltage value whereas the oxidized peaks were shifted towards a more positive voltage value. Furthermore, only the major peak of oxidation and reduction, which was assumed to be the only simple electrode reaction, was studied. The direct electron transfer generation that was accomplished by the *B. piscis* may be the cause of the increase in peak value with scan rate. Also, the relationship between peak current (Ip) and the square root of scan rates ($\upsilon^{1/2}$) for oxidation and reduction peaks was used to calculate the Randles–Sevcik equation (Fig. 7b, c). It was found that the Ip and the $\upsilon^{1/2}$ had a linear relationship. Moreover, the charge transfer at the electrode happens more quickly than the active species diffuse from the bulk solution to the electrode surface. Since, there were narrow, symmetrical faradaic peaks in in CV, the process might have been quick and reversible. The relationship between the peak potential (Ep) and scan rate (log υ) is seen in Fig. 7d, e. The slope values for the log Ip and log υ for the oxidized and reduced peaks were nearly equal (0.35). When *B. piscis* was used as the source of the adsorption processes, the adsorbed nutrients also appeared on the anodic electrode surface. These findings demonstrated that the combination of diffusion and adsorption processes limited the kinetics, demonstrating an irreversible electron charge transfer nature of these peaks [43].

Biofilm characteristic

After the DCMFC operation, the electrode's surface was examined using SEM. A dense biofilm can easily form in the gaps or holes between the electrode's fibers (Fig. 8a). *B. piscis* was rod cells with a cell length ranging between 1.197 and 1.565 μm (Fig. 8a). The bacteria produced aggregates and gathered in groups, supporting the auto-aggregation of the cells following treatment. This suggests that the aggregates are trapped in the fibrils, where they eventually attach and grow. Bacterial adhesion and colonization on the electrode surface would benefit from the mature EPS-based anodic biofilm.

The findings of the EDX elemental mapping displayed in Fig. 8b demonstrated the presence of the elements C, N, O, Na, P, and S. Figure 8c presents the homogeneous distribution of basic elements. According to an elemental analysis, the anodic biofilm contains a higher carbon content than any other element. The coexistence of EPS-BP5M on the bioanode is confirmed by both EDX and elemental mapping.
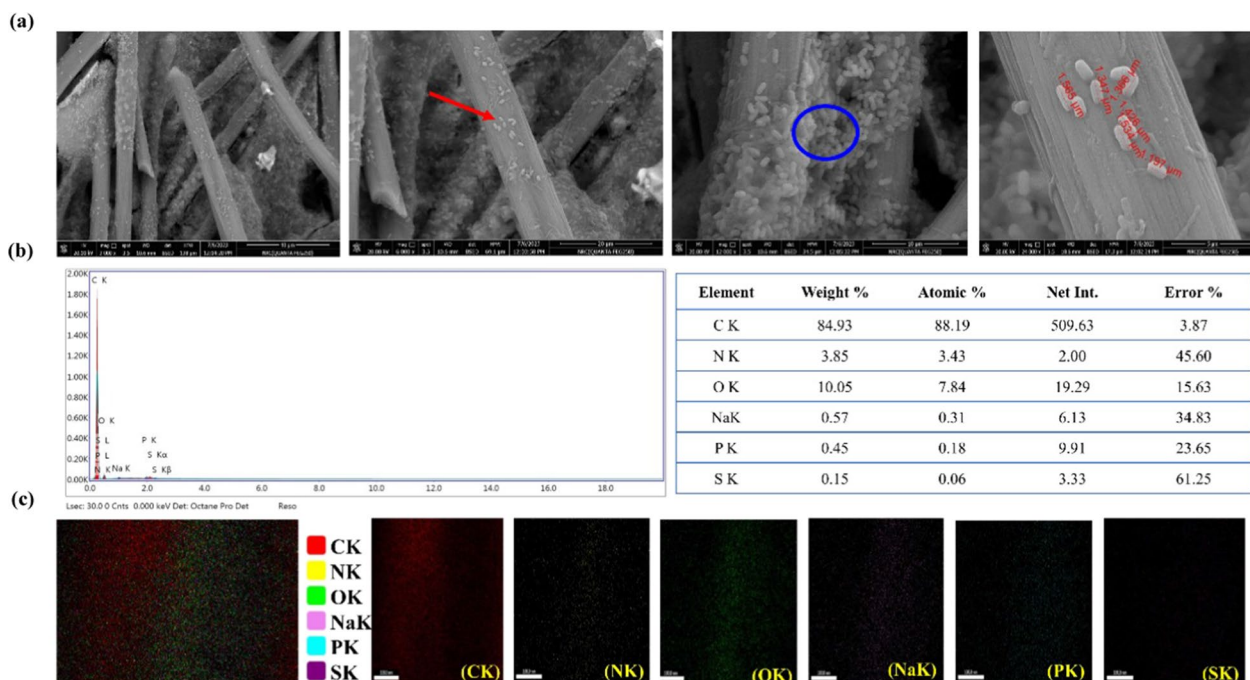
Discussion

Microbial fuel cells (MFC's) are gaining popularity owing to their eco-friendly and energy generation with bioremediation. Molasses are being explored as alternative low-cost nutrients to produce EPS-BP5M by *B. piscis*

Sakr *et al. Microbial Cell Factories* (2023) 22:202

Page 13 of 20
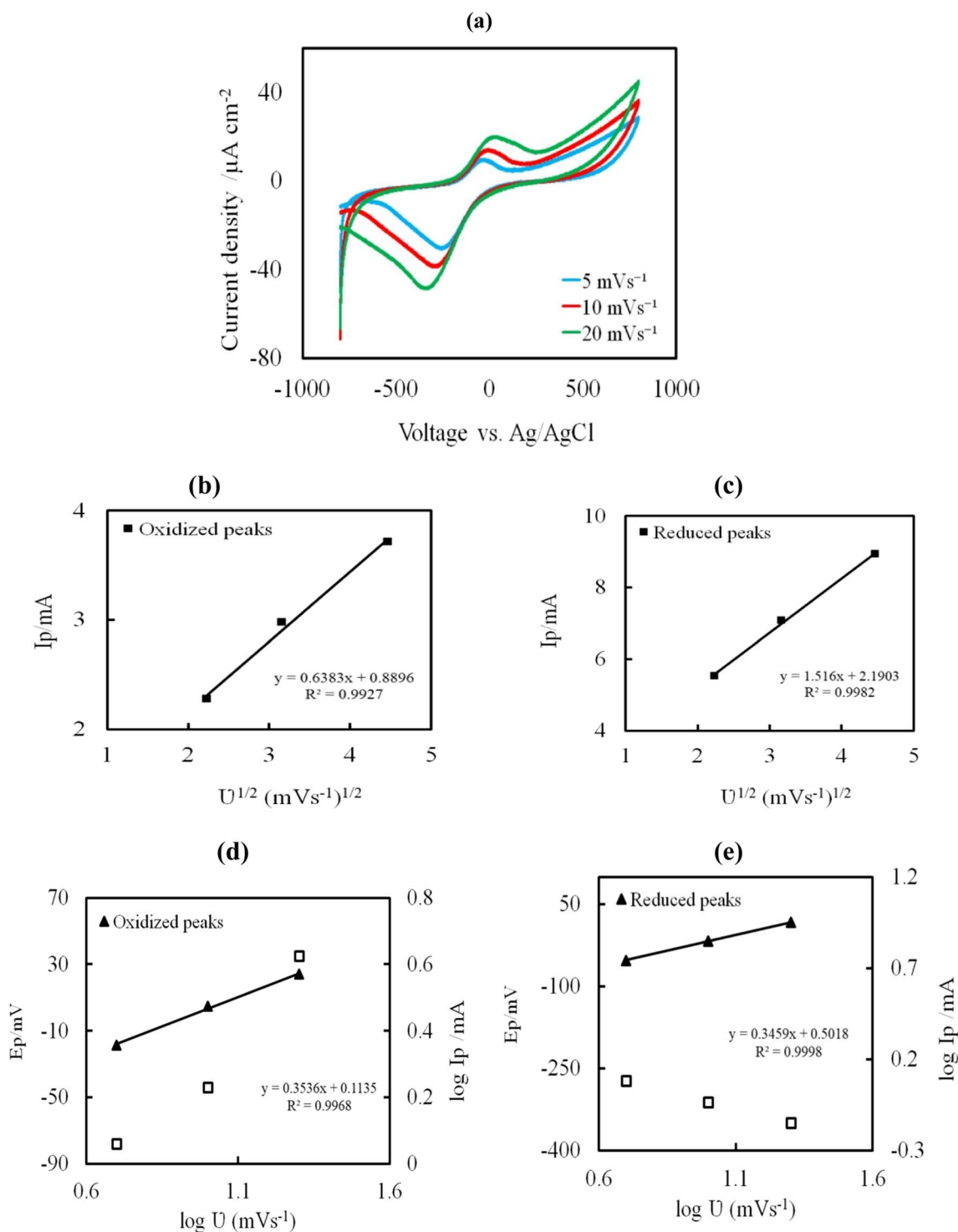
Fig.7 Kinetic study of *B. piscis* oxidation and reduction peaks at the 5th day of inoculation at the scan rates of 5, 10, 20 mV s.$^{-1}$, **a** CV at different scanning rates, **b**, **c** Ip at each redox vs square root of υ (Randles–Sevcik equation), **d**, **e** Ep vs log υ (plain diamonds) and log I vs log υ (black triangles). Ep (peak potential); Ip (peak current); υ (scan rate)

Sakr et al. Microbial Cell Factories (2023) 22:202

Page 14 of 20

Element	Weight %	Atomic %	Net Int.	Error %
C K	84.93	88.19	509.63	3.87
N K	3.85	3.43	2.00	45.60
O K	10.05	7.84	19.29	15.63
NaK	0.57	0.31	6.13	34.83
P K	0.45	0.18	9.91	23.65
S K	0.15	0.06	3.33	61.25

Fig. 8 SEM images taken at different magnifications, bacterial cells (red arrow), bacterial attached to electrode fiber forming aggregates (blue circle) (**a**); EDX analysis (**b**); and elemental mapping (**c**) of biofilm formed on carbon felt anode used in the DCMFC for molasses treatment and electrical power generation

isolated from it (molasses). This study examined the efficiency of *B. piscis* in generating electricity and bioremediate the organic matter from molasses wastewater as anode substrate in DCMFC. To our knowledge, only two papers identified *B. piscis* strain. It was isolated from a *Dissostichus mawsoni* muscle sample from the Antarctic [44] and Indian salterns [45]. Different species of *Bacillus* have been found in the wastes of the sugar industry [46, 47].

Any microbial strain can provide greater yields, but the key is to develop the production medium [48]. Several factors affected the production of EPS including microbial species, culture conditions, and nutritional types [49]. Molasses are useful as a growth medium because they contain high levels of vitamins and minerals and have a strong growth-stimulating impact [50]. It has been utilized as a substrate for the fermentation synthesis of biopolymers because of its various benefits, including high sucrose and other nutrient levels, cheap cost, easy availability, and simplicity of storage [51]. After optimizing the process parameters, the maximum EPS-BP5M production was 27.5 g L^{-1} which is higher than the bacterial EPS gained prior to the use of PBD (5.78 g L^{-1}) by 4.76 times. RSM has been demonstrated to be a useful technique for evaluating the impact of factors on the production of EPS by *B. licheniformis* NS032 [28],

Leuconostoc citreum B-2 [52], and *Pantoea* sp. BCCS 001 GH [31] using molasses as substrate.

A high concentration of minerals and vitamins in molasses, in addition to the sugars that are easily fermented, may be the cause of this increase in productivity [53]. The inhibiting effect of high quantities of mineral components would be mitigated by the diluting of molasses and nitrogen limitation can stimulate the formation of polysaccharides [28]. Bacillus strains that produce EPS are more resilient to environmental stress ([54].

Our findings supported previous findings indicating the carbon source had a significant impact on the formation of EPS [55–57]. The growth of microorganisms and the production of EPS require a carbon source as a substrate. Usually, EPS formation is encouraged by a high concentration of a carbon source [58]. Due to its high sucrose content, molasses was found to have a considerable impact on the EPS-BP5M yield during the screening of growth factors. Bacterial cells might use the additional carbon supply to expand quickly and make more EPS at low concentrations of molasses, but at larger concentrations, catabolite suppression of oxidative pathways will occur, slowing down bacterial development [53, 59], because of an increase in osmotic pressure in the medium, which led to plasmolysis and cell death [53]. Our results indicated that the EPS-BP5M yield from *B.*

Sakr *et al. Microbial Cell Factories* (2023) 22:202

Page 15 of 20

Table 7 Comparisons of current study performance and other similar studies inoculated with molasses wastewater as substrate

MFC construction	Microorganisms used	OCV (mV)	CCV (mV)	Power density	COD %	CE%	References
DCMFC	*Bacillus piscis*	624	265	185.95 mW m^{-2}	90.9	36.9	Current study
H-shape DCMFC	*Meyerozyma guilliermondii*	NA	350	61.25 mW m^{-2}	NA	NA	[1]
SCMFC	Sludge	NA	500	169.86 mW m^{-2}	NA	13.3	[4]
DCMFC	Sludge	NA	7.5	31.37 mW m^{-2}	35.5	NA	[7]
U-shaped DCMFC	Sewage	569	~351	88.9 mW m^{-2}	NA	81	[8]
DCMFC	*Brevibacillus borstelensis*	990	453	188.5 mW m^{-2}	81.7	59.8	[12]
Baffled stacking MFC	Sludge	690		115.5 mW m^{-2}	70	1	[17]
DCMFC	Yeast	NA	372	813.19 mW m^{-2}	97	NA	[62]
SCMFC	*Candida boidinii*	953		5.45W cm^{-2}	NA	NA	[64]
DCMFC	*Pseudomonas Sp*	NA	670	660.82 mW m^{-2}	NA	NA	[72]
DCMFC	Sludge	NA	392	14.9 mW m^{-2}	31.8	6.2	[73]

SCMFC single chamber MFC, *DCMFC* dual chamber MFC, *NA* not applied

piscis is higher than those of other microorganisms such as *Bacillus subtilis* (4.92 g L^{-1}) [53], *Bacillus licheniformis* ANT 179 (16.35 g L^{-1}) [60], *B. licheniformis* mutant strain (9.0 g L^{-1}) [54], and *Pantoea* sp. BCCS001GH (9.9 g L^{-1}) [31].

Auto-aggregation is associated with the development of biofilms [61], which would result if this also happened within our DCMFC. EPS promotes cell aggregation through complicated interactions and also accelerates the development of biofilms and granulation [62]. In the field of wastewater treatment, the ability of microbial cells to auto-aggregate is intriguing as this may encourage the production of bioaggregates and control the efficacy of treatment [63, 64].

Bacillus sp. is simple to grow and produces EPS with a high potential for bioremediation [59]. *B. piscis* was well adapted on the surface of the carbon felt electrode, generating a mature electrogenic biofilm, according to stable voltage outputs [3, 17]. The power density for the present study was found to be comparable with many of the reported literature values as shown in Table 7. The PD$_{max}$ values were higher than those examined by Fan et al. (2016). They utilized a DCMFC fueled with simulated molasses wastewater as the anode substrate and showed PD$_{max}$ generation of 31.37 mW m^{-2} with a matching voltage output of about 7.5 mV [7]. Additionally, Lee et al. (2016) reported in another investigation that the DCMFC's highest CD was 80 mA m^{-2} and PD was 17 mW m^{-2} [65]. In contrast, our finding was lower than the research conducted by Syafitri et al. (2018). They reported that the DCMFC produced the maximum voltage (0.372 V) and PD$_{max}$ (813.191 mW m^{-2}) when sediment was mixed with molasses [66]. The discrepancy in power density values revealed in various publications may be due to variations in substrates, microbial species, MFC configuration, electrode materials, and PEMs. Our novel *B. piscis* exhibits good performance on electricity generation using molasses wastewater as anode fuel.

As the COD concentrations decreased, the overall COD removal efficiency increased yields by 54.55, 63.64, and 90.91%, respectively. These findings suggested that the *B. piscis* activity is more potent and may be employed for COD elimination and voltage generation from molasses [3, 67]. The fermentation mechanisms, biomass formation, and consumption of coulombs during methanogenesis, which take place in the anode chamber through the breakdown of a portion of molasses, could be the cause of the reduction of CE in the MFC [68].

Molasses wastewater has a dark brown color due to the presence of amounts of melanoidins, caramel, and phenolic pigments present. Melanoidins are the hardest to get rid of because it has the largest content and most complex structure of all of them [69]. After DCMFC treatment, a decolorization rate can break down complex compounds like melanoidoin, producing colorless intermediate metabolites [70]. The rates of decolorization in the current study are higher than those previously reported by Mohanakrishna et al. [71], who reported 22.92% of decolorization following MFC treatment of distillery effluent inoculated with mixed consortia.

B. piscis' electrocatalytic activity is supported to regulate subsequent oxidation processes and intermediate breakdown [12]. The linear relationship of Ip and the $\upsilon^{1/2}$ indicated the performance was subjected to a diffusion-controlled process [72]. Excellent and efficient adsorption occurs through the electrode holes because it enhances the contact between pollutants and exoelectrogens [73]. Bacterial adhesion and colonization on the electrode surface would benefit from the mature EPS-based anodic biofilm. Consequently, it might be said that the bacteria were metabolically active and increased power output [74].

Sakr *et al. Microbial Cell Factories* (2023) 22:202

Page 16 of 20

Conclusions

In the present study, a novel EPS-producing bacteria, *B. piscis*, was isolated and identified from molasses waste. The efficient EPS-BP5M production in an optimized medium with inexpensive sugarcane molasses substrate was also carried out which resulted in higher EPS-BP5M production. To stick to the carbon felt electrode of the DCMFC, the bacterium most likely generates EPS-BP5M. This work offered new insights on the use of bacteria that produce EPS using molasses. EPS-BP5M was characterized using FT-IR, NMR, and HPLC. *B. piscis* could be used as an anodic biocatalyst for the treatment of sugar industry molasses used as a substrate in a DCMFC and simultaneous energy recovery. Our findings show an effective and eco-friendly approach (DCMFC) that uses molasses, a sustainable agricultural by-product, to solve the problem of eliminating organic matter and producing bioelectricity.. Further work will be done on molasses wastewater treatment.

Material and methods

Collection and analysis of sugarcane molasses

The sugar company for integrated industries, located in Hawamdiya, Giza, Egypt, kindly donated the sugarcane molasses. The collected material was carried to the lab with care, stored immediately at 4 °C, and then brought to room temperature before usage. According to the Association of Official Analytical Chemists (AOAC) guidelines, the chemical composition was examined [75].

Isolation of EPS producing bacteria

First, Erlenmeyer flasks holding 25 mL of liquid nutrient broth (NB) medium were inoculated with 1.0 mL of sugarcane molasses and incubated at 37 °C for 48 h. Then, 1.0 mL of that culture was transported to petri dishes with nutrient agar medium amended with 1% sucrose and incubated for 48 h at 37 °C. Striking was used to separate the mucoid colonies into pure cultures, which were then frozen at −20 °C in NB medium with 25% glycerol.

EPS production, extraction, and purification

Bacterial isolates were screened for their ability to produce EPS by inoculation of NB medium supplemented with 1% sucrose. Then, the inoculated flasks were incubated at 37 °C for 48 h. The fermentation broth was centrifuged at 6000 rpm for 10 min, and the supernatant was then mixed with Savage reagent (chloroform: *n*-butanol, 2:1 v/v). The organic layer was recovered, combined at a ratio of 1:3 (v/v) with cold absolute ethanol, and then left to stand at 4 °C overnight. The precipitate was collected and mixed with ultrapure water to create a crude EPS solution. This solution underwent a 72-h dialyze in deionized water to produce an EPS. For the following trials, the isolate that produced the highest yield of EPS was chosen.

Molecular analysis of the selected EPS producing isolate

Using 16S rRNA gene sequencing, the chosen bacteria were identified. Using universal 16S rDNA primers, the extracted and purified DNA was amplified. The amplified product was sequenced and deposited into the NCBI database. The bacterial sequence was submitted to the GenBank database and the accession number was obtained. The isolated bacteria were then aligned, and MEGA software version 11 was used to create phylogenetic trees using the neighbor joining method.

Molasses-based media optimization

Pretreatment of molasses

Molasses used as a carbon source were mixed with distilled water containing 2% sodium dihydrogen phosphate (1:1). The solution was autoclaved at 121 °C for 10 min before being allowed to cool for 24 h. Clarified molasses was the only source of carbon used [76].

Fermentation media

During the fermentation procedure, a 250 mL flask was filled with 100 mL of medium. The production medium's composition varied depending on the experimental approach outlined below. Depending on the experimental design, the best isolate (50×10^6 CFU/mL) was employed to inoculate the sterilized medium. The cultivation process took place at 37 °C for 48 h. In order to calculate the yield of EPS-BP5M (g L^{-1}) at the end of the fermentation, samples from the liquid culture were taken.

Experimental designs

PBD was used to organize 11 independent variables at two levels with 12 runs to rank the impact of various factors on EPS-BP5M yield (Table 2). The tested variables were molasses, yeast extract, peptone extract, NaCl, KH_2PO_4, K_2HPO_4, $NaNO_3$, $MgSO_4$, $MgCl_2$, inoculum size, and pH.

According to the PBD experiment, molasses, $MgSO_4$, and inoculum size were further optimized using the RSM. As shown in Table 4, variables were performed at three-level (low, middle, and high) trials. Design-Expert software created a 17-run experimental design scheme in accordance with the coding design, utilizing the yield of EPS-BP5M (Y) as the response value at the end of fermentation.

Design-Expert 7.0 software was used to output the results of variance analysis of the PBD experiment and Box–Behnken experiment and carry out regression

Sakr *et al. Microbial Cell Factories* (2023) 22:202

Page 17 of 20

analysis of the results of the Box–Behnken experiment to simulate the prediction equation.

Structural characterization

Ultraviolet–visible (UV–Vis) spectroscopy of the sample was evaluated using a Shimadzu UV-1800 UV spectrophotometer with a wavelength range of 200–600 nm. Using an FTIR (Bruker Alpha 11), the EPS-BP5M sample's functional group content was initially validated. One mg of the sample was combined directly with KBr and then quantified using a spectrum. EPS-BP5M's. ^{1}H-NMR spectrum was obtained utilizing a BRUKER 400 MHz spectrometer at 25 °C. Following that, the material was dissolved in D_2O at a 50 mg/mL concentration. Parts per million (ppm) were used to describe chemical changes. The EURO EA Elemental Analyzer was used to conduct an elemental analysis on the carbon, hydrogen, nitrogen, and sulphur weight percentages of EPS-BP5M. Approximately 1.0 mg of the material was burned. Gas chromatography is used to quantify the combustion byproducts (C, H, N, and S), and the ratio of the original sample's constituents is then calculated.

Monosaccharide composition

The monosaccharide compositions were analyzed by HPLC using a Shim-pack SCR-101N column with a mobile phase of ultrapure water. A paste was made by carefully adding 0.5 ml of ice-cold 80% H_2SO_4 to the EPS-BP5M sample. After that, the paste was carefully mixed for 15 h at room temperature. The paste was then diluted with a solution of ice and distilled water (up to 6.5 mL) until the sulfuric acid strength reached 2N. The solution was further hydrolyzed for 6 h in a sealed tube over a boiling water bath. The hydrolyzate that was produced was neutralized by $BaCO_3$ before being filtered and thoroughly rinsed with water. After that, a cation exchange resin (Amberlite IR-120 (H+)) was used to treat the filtrate and washings. A flow rate of 0.7 ml/min was used to analyze the monosaccharide content. After integrating the relevant areas and comparing the results to standard curves made from glucose, fructose, sucrose, and arabinose (Sigma), each carbohydrate concentration was calculated.

Bacterial surface properties

Three subcultures of the isolate were performed in NB medium at 37 °C. After centrifuging the active cultures for 5 min at 6000 rpm, they were washed with sterile saline solution. The washed pellets were combined with sterilized phosphate-buffered saline (PBS) buffer for autoaggregation [77] or saline solution for hydrophobicity [78], and the OD_{600} nm was adjusted (A_0, H_0). For the auto-aggregation assay, the bacterial culture (8 mL) was incubated at 37 °C, and the auto-aggregation values were recorded at 3, 6, and 24 h (A_t). It was determined using the equation (%) = 100

* $[1 - (A_t/A_0)]$. To determine the hydrophobicity of the cell surface, hexadecane was employed as a solvent. The cell suspension was mixed with hexadecane, and the process was vortexed for 1.0 min. A_t 600 nm (H_1), the optical density of the aqueous phase was determined after 15 min of separation. The equation affinity (%) = 100 * $[1 - (H_1/H_0)]$ was then used to compute the percentage of cells that were transported to the hexadecane phase.

Synergistic interactions of DCMFC and microbially induced removal of color and COD of molasses waste as the substrate

DCMFC construction and operation

The experimental system was mainly made up of a dual-chamber MFC reactor that was assembled by joining two cylindrical plexiglass chambers that served as the anodic and cathodic chambers. These chambers were 6 cm long, 4.6 cm in diameter, and had a total working volume of 100 mL. Proton exchange membrane (PEM, Nafion 117, Dupont Co.), which assures the transmission of only hydrogen ions and no other ions, was used as the separator between the anode and cathode. The anode comprised an unmodified sheet of three-dimensional carbon felt joined to the top of an externally connected anode port with affective dimensions of 2.5×2.5×0.6 cm and a projected surface area of 18.50 cm^2. The cathodic electrode was made of non-waterproof gas diffusion carbon cloth with a microporous sheet (6×6 cm each; surface area equivalent to 16.63 cm^2). A stainless steel wire was used to link the electrodes in bioreactors so that electrons could be transferred. A 50 mM phosphate buffer solution was employed in the cathode chamber, which was left open to the atmosphere for ventilation of O_2 as an electron acceptor, while the anode chamber was completely sealed with epoxy sealant to maintain an anaerobic environment [42, 79]. The anode substrate was obtained in fed-batch mode using the molasses wastewater (g L^{-1}) with 50 mL as the carbon source, 2.0 g yeast extract, 2.0 g peptone, 0.5 g NaCl, 0.1 g KH_2PO_4, 1.0 g K_2HPO_4, 2.5 g $NaNO_3$, 0.5 g $MgSO_4$, 0.5 g $MgCl_2$, and 4% inoculum size. The electrolyte was adjusted to pH 7 with NaOH. *B. piscis* that had first been activated overnight in NB medium was inoculated into DCMFC to aid in the breakdown of molasses. The strain was cultivated in 100 mL of NB medium for 24 h at 37 °C, followed by a 10-min centrifugation at 6000 rpm at 4 °C. Phosphate-buffered saline (PBS) was used to wash the cell pellets before they were adjusted to 50×10^6 CFU/mL. After the sugarcane molasses was consumed and the decline phase, fresh *B. piscis* and molasses were added to the anodic. The experiments were run at room temperature.

Sakr *et al. Microbial Cell Factories*　(2023) 22:202

Page 18 of 20

DCMFC analysis and calculations

The voltage of the DCMFC was recorded every 5 min using a data acquisition system (Lab jack U6-PRO) connected to a laptop, and Ohm's Law (V = IR) was used to determine the current value when the external resistance was set to 10 kΩ. Open circuit voltage (OCV), which was obtained in the steady state when the circuit was opened. Polarization and power curves were generated by manually stepping down the external resistance from 650,000 to 100 Ω. The current and power was normalized to the anode surface area to calculate the current density (mA m^{-2}) and power density (mW m^{-2}). Internal resistance is determined by the slope of the linear region of the current–voltage graph. According to APHA standard procedures, COD concentrations in influent and effluent were evaluated. Organic concentrations were estimated as COD removal efficiency (COD R%), which was calculated using the following equation: COD R % = 100 * [(COD$_{initial}$ − COD$_{final}$)/COD$_{initial}$], where COD$_{initial}$ is the COD concentration in the influent (mg COD/L), and COD$_{final}$ is the COD concentration in the final effluent at the end of DCMFC batch cycles (mg COD/L) [4]. The coulombic efficiency (C$_E$) expresses the charge efficiency in which electrons were being transferred in the DCMFC. It was calculated by dividing the generated current to the theoretical current as CE = [$M \int I.dt$ / nFvΔCOD] * 100, where I is current output (A), v is the working volume (L) in the anode, n is the number of electrons exchanged per mole of O$_2$ = 4, F is Faraday's constant (96,485 A s mol^{-1}), ΔCOD is change in chemical oxygen demand (g L^{-1}), M the molar weight of oxygen [8].

Color removal

After DCMFC treatment, molasses samples were diluted 1:10 in triplicate, the pH was set to 7.0, and they were then subjected to a spectral scan by the UV-1800 spectrophotometer from wavelengths between 350 and 650 nm to assess the decolorization. The formula used to determine color removal efficiency (ξcolor %) at 475 nm (the wavelength at which melanoidins absorb best) is ξcolor % = 100 * [1 − (A$_i$/A$_f$)], where A$_i$ and A$_f$ refer to initial and final absorbance, respectively. The samples were taken after each cycle to measure the color [70].

The electrochemical measurements

Cyclic voltammetry (CV) of sterilized DCMFC that inoculated with a single culture of *B. piscis* (cell suspension of 50×10^6 CFU mL^{-1} at logarithmic phase) was achieved by applying various scan rates at 5, 10, and 20 m mV s^{-1} at different testing periods from 24 to 288 h after cell operation. The CVs were collected using the Voltamaster 6 potentiostat (PST006) in the potential range of − 0.8 to 0.8 V vs. Ag/AgCl. The anode, cathode, and Ag/AgCl (Metrohm) were implemented as working, counter, and reference electrodes, respectively. The study of the reversibility of the electron transfer was depicted by the peak potential dependence on scan rate and linearity of the Randles–Sevcik equation (linear plot of peak current dependence on the square root of scan rate) [80].

Biofilm characterization

Using scanning electron microscopy (SEM Quanta FEG 250 with field emission gun, FEI Company, Netherlands), the surface morphologies and microstructures of the anodic biofilm were studied. The biofilm was performed by fixing in 0.1 M phosphate buffer (pH 7.0) containing 2.5% (v/v) glutaraldehyde for an overnight period [81]. The increasing gradients of ethanol (25, 50, 70, and 100%) were used to induce dehydration. The biofilm was allowed to dry at room temperature before being sputter-coated with gold and subjected to analysis at a voltage 20 kV. Additionally, energy-dispersive X-ray spectroscopy (EDX) was used to determine the element content and elemental distribution maps.

Statistical analysis

The statistical analysis was done using the Microsoft Excel 2016 version. Data analysis dealt with all variables, computations, means, and standard deviations.

Data availability
All data generated or analyzed during this study are included in this article.

Declarations

Ethics approval and consent to participate
This study was approved by the Ethics Committee of Women Faculty for Arts, Science, and Education, Ain Shams University, Cairo, Egypt.

Consent for publication
Approved by all named authors.

Competing interests
The authors declare that they have no competing interests.

Author details
[1]Botany Department, Faculty of Women for Arts, Science and Education, Ain Shams University, Cairo, Egypt. [2]Chemical Engineering and Pilot Plant Department, National Research Centre (NRC), El Buhouth St., Cairo 12622, Dokki, Egypt.

Sakr *et al. Microbial Cell Factories* (2023) 22:202

Page 19 of 20

References

1. Zohri AEA, Hassan SHA, Rehab MF. Potentiality of some yeast isolates for electricity generation from sugarcane molasses. Egypt Sugar J. 2018;11:71–84.
2. Badawi EY, Elkharsa RA, Abdelfattah EA. Value proposition of bio-hydrogen production from different biomass sources. Energy Nexus. 2023;10:100194.
3. Öztürk M, Onat TA. The usage of molasses and mediators in microbial fuel cells. JOTCSB. 2017;5:77–84.
4. Hu X, Liu J, Cheng W, Li X, Zhao Y, Wang F, et al. Synergistic interactions of microbial fuel cell and microbially induced carbonate precipitation technology with molasses as the substrate. Environ Res. 2023;228:115849.
5. Roy H, Rahman TU, Tasnim N, Arju J, Rafid MM, Islam MR, et al. Microbial fuel cell construction features and application for sustainable wastewater treatment. Membranes (Basel). 2023;13:490.
6. Rahman A, Borhan MS, Rahman S. Evaluation of microbial fuel cell (MFC) for bioelectricity generation and pollutants removal from sugar beet processing wastewater (SBPW). Water Sci Technol. 2018;1:387–97.
7. Fan L, Xu D, Li C, Xue S. Molasses Wastewater treatment by microbial fuel cell with MnO$_2$-modified cathode. Pol J Environ Stud. 2016;25:2359–2356.
8. Javed MM, Nisar MA, Ahmad MU. Effect of NaCl and pH on bioelectricity production from vegetable waste extract supplemented with cane molasses in dual chamber microbial fuel cell. Pak J Zool. 2022;54:247–54.
9. Abubackar HN, Biryol I, Ayol A. Yeast industry wastewater treatment with microbial fuel cells: effect of electrode materials and reactor configurations. Int J Hydrogen Energy. 2023;48:12424–32.
10. Choudhury P, Majumdar R, Bandyopadhyaya TK. Comparative study between synthetic and dairy wastewaters in single chamber microbial fuel cell for power generation. J Electrochem Sci Eng. 2021;11:279–89.
11. Chen T, Zhang S, Yuan Z. Adoption of solid organic waste composting products: a critical review. J Clean Prod. 2020;272:122712.
12. Hassan SHA, Zohri NA, Kassim RMF. Electricity generation from sugarcane molasses using microbial fuel cell technologies. Energy. 2019;178:538–43.
13. Wang Y, Guo W, Xing D, Chang J. Hydrogen production using biocathode single-chamber microbial electrolysis cells fed by molasses wastewater at low temperature. Int J Hydrogen Energy. 2014;39:19369–75.
14. Tyagi B, Gupta B, Khatak D, Meena R, Thakur IS. Genomic analysis, simultaneous production, and process optimization of extracellular polymeric substances and polyhydroxyalkanoates by Methylobacterium sp. ISTM1 by utilizing molasses. Bioresour Technol. 2022;354:127204.
15. Lee Y-Y, Kim TG, Cho K-S. Characterization of the COD removal, electricity generation, and bacterial communities in microbial fuel cells treating molasses wastewater. J Environ Sci Health A. 2016;51:1131–8.
16. Zhang B, Zhao H, Zhou S, Shi C, Wang C, Ni J. A novel UASB–MFC–BAF integrated system for high strength molasses wastewater treatment and bioelectricity generation. Bioresour Technol. 2009;100:5687–93.
17. Zhong C, Zhang B, Kong L, Ni J. Electricity generation from molasses wastewater by an anaerobic baffled stacking microbial fuel cell. J Chem Technol Biotechnol. 2011;86:406–13.
18. Asefi B, Li S-L, Moreno HA, Sanchez-Torres V, Hu A, Li J, et al. Characterization of electricity production and microbial community of food waste-fed microbial fuel cells. Process Saf Environ Prot. 2019;125:83–91.
19. Angelaalincy MJ, Navanietha Krishnaraj R, Shakambari G, Ashokkumar B, Kathiresan S, Varalakshmi P. Biofilm engineering approaches for improving the performance of microbial fuel cells and bioelectrochemical systems. Front Energy Res. 2018;6:63.
20. Yin W, Wang Y, Liu L, He J. Biofilms: the microbial "protective clothing" in extreme environments. Int J Mol Sci. 2019;20:3423.
21. Caruso C, Rizzo C, Mangano S, Poli A, Di Donato P, Finore I, et al. Production and biotechnological potential of extracellular polymeric substances from sponge-associated Antarctic bacteria. Appl Environ Microbiol. 2018;84:e01624-e1717.
22. Asgher M, Urooj Y, Qamar SA, Khalid N. Improved exopolysaccharide production from *Bacillus licheniformis* MS3: optimization and structural/functional characterization. Int J Biol Macromol. 2020;151:984–92.
23. Ma L, Guo X, Yang J, Zeng X, Ma K, Wang L, et al. Characterization and antibacterial activity of a polysaccharide produced from sugarcane molasses by *Chaetomium globosum* CGMCC 6882. Front Nutr. 2022;9:935632.
24. Singh RS, Kaur N, Kennedy JF. Pullulan production from agro-industrial waste and its applications in food industry: a review. Carbohydr Polym. 2019;217:46–57.
25. Acosta SBP, Marchioro MLK, Santos VAQ, Calegari GC, Lafay CBB, Barbosa-Dekker AM, et al. Valorization of soybean molasses as fermentation substrate for the production of microbial exocellular β-glucan. J Polym Environ. 2020;28:2149–60.
26. Li Q, Zhou Y, Ke C, Bai Y, Liu X, Li S. Production of welan gum from cane molasses by Sphingomonas sp. FM01. Carbohydr Polym. 2020;244:116485.
27. Song Y-R, Jeong D-Y, Baik S-H. Optimal production of exopolysaccharide by Bacillus licheniformis KS-17 isolated from kimchi. Food Sci Biotechnol. 2013;22:417–23.
28. Gojgic-Cvijovic GD, Jakovljevic DM, Loncarevic BD, Todorovic NM, Pergal MV, Ciric J, et al. Production of levan by *Bacillus licheniformis* NS032 in sugar beet molasses-based medium. Int J Biol Macromol. 2019;121:142–51.
29. Wang Z, Zhou F, Quan Y. Antioxidant and immunological activity in vitro of polysaccharides from *Phellinus nigricans* mycelia. Int J Biol Macromol. 2014;64:139–43.
30. Wang Y, Du R, Qiao X, Zhao B, Zhou Z, Han Y. Optimization and characterization of exopolysaccharides with a highly branched structure extracted from *Leuconostoc citreum* B-2. Int J Biol Macromol. 2020;142:73–84.
31. Niknezhad SV, Kianpour S, Jafarzadeh S, Alishahi M, Najafpour Darzi G, Morowvat MH, et al. Biosynthesis of exopolysaccharide from waste molasses using Pantoea sp. BCCS 001 GH: a kinetic and optimization study. Sci Rep. 2022;12:10128.
32. Zhu G, Sheng L, Tong Q. Preparation and characterization of carboxymethyl-gellan and pullulan blend films. Food Hydrocoll. 2014;35:341–7.
33. Ahuja M, Singh S, Kumar A. Evaluation of carboxymethyl gellan gum as a mucoadhesive polymer. Int J Biol Macromol. 2013;53:114–21.
34. Lule VK, Singh R, Pophaly SD, Poonam, Tomar SK. Production and structural characterisation of dextran from an indigenous strain of *Leuconostoc mesenteroides* BA 08 in whey. Int J Dairy Technol. 2016;69:520–31.
35. Liu Q, Yu S, Zhang T, Jiang B, Mu W. Efficient biosynthesis of levan from sucrose by a novel levansucrase from *Brenneria goodwinii*. Carbohydr Polym. 2017;157:1732–40.
36. Fox CA, Abdulla HA, Burdige DJ, Lewicki JP, Komada T. Composition of dissolved organic matter in pore waters of anoxic marine sediments analyzed by 1H nuclear magnetic resonance spectroscopy. Front Mar Sci. 2018;5:172.
37. Zhang P, Yang C, Xu Y, Li H, Shi W, Xie X, et al. Accelerating the startup of microbial fuel cells by facile microbial acclimation. Bioresour Technol Rep. 2019;8:100347.
38. Sirinutsomboon B. Modeling of a membraneless single-chamber microbial fuel cell with molasses as an energy source. Int J Energy Env Eng. 2014;93:2–9.
39. Hubenova Y, Mitov M. Extracellular electron transfer in yeast-based biofuel cells: a review. Bioelectrochemistry. 2015;106:177–85.
40. Yaakop AS, Ahmad A, Hussain F, Oh S, Alshammari MB, Chauhan R. Domestic organic waste: a potential source to produce the energy via a single-chamber microbial fuel cell. Int J Chem Eng. 2023;2023:1–10.
41. Ahmad A. Conventional vegetable waste: a potential source for the high performance of benthic microbial fuel cells. Biomass Convers Biorefin. 2023;1–13. https://doi.org/10.1007/s13399-023-04447-8
42. Manjerkar Y, Kakkar S, Durve-gupta A. Bio-electricity generation using kitchen waste and molasses powered MFC. IJSRSET. 2018;5:181–7.
43. Shoparwe NF, Makhtar MMZ, Sata SA, Kew WS, Mohamad M, Shukor H. Cyclic voltammetry studies of bioanode microbial fuel fells from batch culture of *Geobacter sulfurreducens*. Earth Environ Sci. 2021;765:012102.
44. Lee J-B, Jeon SH, Choi S-G, Jung H-Y, Kim MK, Srinivasan S. *Bacillus piscis* sp. nov., a novel bacterium isolated from the muscle of the antarctic fish *Dissostichus mawsoni*. J Microbiol. 2016;54:809–13.
45. Rathakrishnan D, Gopalan AK. Isolation and characterization of halophilic isolates from Indian salterns and their screening for production of hydrolytic enzymes. Environ Challenges. 2022;6:100426.

Sakr *et al. Microbial Cell Factories* (2023) 22:202

Page 20 of 20

46. Córdova-Bautista Y, Ramirez-Morales E, Perez-Hernandez B, Ojeda-Morales ME, Lopez-Lazaro JS, Martinez-Pereyra G. Electricity production and bioremediation from synthetic sugar industry wastewater by using microbial isolate in microbial fuel cell. Sugar Technol. 2020;22:820–9.

47. Singh G, Kumari A, Mittal A, Yadav A, Aggarwal NK, et al. Poly β-hydroxybutyrate production by *Bacillus subtilis* NG220 using sugar industry waste water. Biomed Res Int. 2013;2013:1–10.

48. Farahat M. Enhancement of β-Cyclodextrin Production and Fabrication of Edible Antimicrobial Films Incorporated with Clove Essential Oil/β-cyclodextrin Inclusion Complex. Microbiol Biotechnol Lett. 2020;48:12–23. https://doi.org/10.4014/mbl.1909.09016.

49. Hou C, Yin M, Lan P, Wang H, Nie H, Ji X. Recent progress in the research of *Angelica sinensis* (Oliv.) Diels polysaccharides: extraction, purification, structure and bioactivities. Chem Biol Technol Agric. 2021;8:1–14.

50. Onbasli D, Aslim B. Determination of antimicrobial activity and production of some metabolites by *Pseudomonas aeruginosa* B1 and B2 in sugar beet molasses. Afr J Biotechnol. 2008;7:4614–19.

51. Mao YL, Tian CX, Zhu JW, Zhang TZ, Tong LB. Production of a novel biopolymer by culture of *Bacillus cereus* B-11 using molasses wastewater and its use for dye removal. Adv Mater Res. 2011;230:1119–22.

52. Liang L, Xu M, Pan L, Zhou Z, Han Y. Structural characterization of exopolysaccharide produced by *Leuconostoc citreum* B-2 cultured in molasses medium and its application in set yogurt. Processes. 2022;10:891.

53. Razack SA, Velayutham V, Thangavelu V. Medium optimization for the production of exopolysaccharide by *Bacillus subtilis* using synthetic sources and agro wastes. Turk J Biol. 2013;37:280–8.

54. Asgher M, Rani A, Khalid N, Qamar SA, Bilal M. Bioconversion of sugarcane molasses waste to high-value exopolysaccharides by engineered *Bacillus licheniformis*. Case Stud Chem Environ Eng. 2021;3:100084.

55. Qamar SA, Asgher M, Bilal M. Sustainable production, optimization, and partial characterization of exopolysaccharides by *Macrococcus brunensis*. Waste Biomass Valoriz. 2021;12:6847–59.

56. Sathishkumar R, Thirumalaikumar E, Rajeswari MV, Arun J, Vimal S, Babu MM, et al. Extraction, statistical optimization, and immunomodulatory activity of exopolysaccharide from seaweed-associated *Bacillus megaterium* DSKPDF CMST3. Biomass Convers Biorefinery. 2022;1–14. https://doi.org/10.1007/s13399-021-02180-8

57. Tilwani YM, Lakra AK, Domdi L, Yadav S, Jha N, Arul V. Optimization and physicochemical characterization of low molecular levan from *Enterococcus faecium* MC-5 having potential biological activities. Process Biochem. 2021;110:282–91.

58. Karadayi YI, Aykutoglu G, Arslan NP, Baltaci MO, Adiguzel A, Taskin M. Production of water-soluble sulfated exopolysaccharide with anticancer activity from *Anoxybacillus gonensis* YK25. J Chem Technol Biotechnol. 2021;96:1258–66.

59. Kalpana R, Angelaalincy MJ, Kamatchirajan BV, Vasantha VS, Ashokkumar B, Ganesh V, et al. Exopolysaccharide from *Bacillus cereus* VK1: enhancement, characterization and its potential application in heavy metal removal. Colloids Surf B Biointerfaces. 2018;171:327–34.

60. Xavier JR, Ramana KV. Optimization of levan production by cold-active *Bacillus licheniformis* ANT 179 and fructooligosaccharide synthesis by its levansucrase. Appl Biochem Biotechnol. 2017;181:986–1006.

61. Soh SM, Lee D-G, Mitchell RJ. Enhanced microbial fuel cell (MFC) power outputs through membrane permeabilization using a branched polyethyleneimine. Biosens Bioelectron. 2020;170:112623.

62. Nouha K, Kumar RS, Balasubramanian S, Tyagi RD. Critical review of EPS production, synthesis and composition for sludge flocculation. J Environ Sci. 2018;66:225–45.

63. Purba LDA, Ibiyeye HT, Yuzir A, Mohamad SE, Iwamoto K, Zamyadi A, et al. Various applications of aerobic granular sludge: a review. Environ Technol Innov. 2020;20:101045.

64. Wang X, An Q, Zhao B, Guo JS, Huang YS, Tian M. Auto-aggregation properties of a novel aerobic denitrifier Enterobacter sp. strain FL. Appl Microbiol Biotechnol. 2018;102:2019–30.

65. Lee Y, Kim TG, Cho K. Characterization of the COD removal, electricity generation, and bacterial communities in microbial fuel cells treating molasses wastewater communities in microbial fuel cells treating molasses. J Environ Sci Health Part A. 2016;46:1–8.

66. Syafitri LM, Saputro YA, Hana PN, Hardiani D, Raharjo B. Bioelectric production from sediment of pond fishing and molasses using microbial fuel cell (MFC) technology-base with the influence of substrate concentration

67. Flores SR, Pérez-Delgado O, Naveda-Renny N, Benites SM, De La Cruz-Noriega M, Narciso DAD. Generation of bioelectricity using molasses as fuel in microbial fuel cells. Environ Res Eng Manag. 2022;78:19–27.

68. Rahman A, Borhan MS, Rahman S. Evaluation of microbial fuel cell (MFC) for bioelectricity generation and pollutants removal from sugar beet processing wastewater (SBPW). Water Sci Technol. 2018;77:387–97.

69. Gökçek ÖB, Sarıoğlu M, et al. Anaerobic treatment of the mixture of automotive industry and molasses wastewater for different organic loading rates in an upflow anaerobic sludge blanket (UASB) reactor. Desalin Water Treat. 2018;105:83–91.

70. Marassi RJ, Igreja M, Uchigasaki M, Silva GC. High strength bioethanol wastewater inoculated with single-strain or binary consortium feeding air-cathode microbial fuel cells. Environ Prog Sustain Energy. 2019;38:380–6.

71. Mohanakrishna G, Mohan SV, Sarma PN. Bio-electrochemical treatment of distillery wastewater in microbial fuel cell facilitating decolorization and desalination along with power generation. J Hazard Mater. 2010;177:487–94.

72. Pinto AMFR. Cyclic voltammetry study of a yeast-based microbial fuel cell. Bioresour Technol Rep. 2022;17:100974.

73. Flores BD, Flores IV, Guerrero A, Orellana DR, Pohlmann JG, Diez MA, et al. Effect of charcoal blending with a vitrinite rich coking coal on coke reactivity. Fuel Process Technol. 2017;155:97–105.

74. Salar-Garcìa MJ, Gajda I, Ortiz-Martìnez VM, Greenman J, Hanczyc MM, de Los Rios AP, et al. Microalgae as substrate in low cost terracotta-based microbial fuel cells: novel application of the catholyte produced. Bioresour Technol. 2016;209:380–5.

75. Horwitz WP, editor. Official methods of analysis. Association of Official Analytical Chemists. Inc, Arlingt. 1980;1:2.

76. Prasanna PHP, Grandison AS, Charalampopoulos D. Bifidobacteria in milk products: an overview of physiological and biochemical properties, exopolysaccharide production, selection criteria of milk products and health benefits. Food Res Int. 2014;55:247–62.

77. Zuo F, Yu R, Feng X, Chen L, Zeng Z, Khaskheli GB, et al. Characterization and in vitro properties of potential probiotic Bifidobacterium strains isolated from breast-fed infant feces. Ann Microbiol. 2016;66:1027–37.

78. Kouzuma A, Meng X-Y, Kimura N, Hashimoto K, Watanabe K. Disruption of the putative cell surface polysaccharide biosynthesis gene SO3177 in *Shewanella oneidensis* MR-1 enhances adhesion to electrodes and current generation in microbial fuel cells. Appl Environ Microbiol. 2010;76:4151–7.

79. Baharuddin M, Rajib M, Zahra U. Effect of combination of electrolyte and buffer on electrical production in fuel cell microbial system with Pseudomonas sp. in molasses substrate. E3S Web Conf. 2020;03001:1–7.

80. Peixoto L, Parpot P, Martins G. Assessment of electron transfer mechanisms during a long-term sediment microbial fuel cell operation. Energies. 2019;12:481.

81. La JA, Jeon J-M, Sang B-I, Yang Y-H, Cho EC. A hierarchically modified graphite cathode with Au nanoislands, cysteamine, and Au nanocolloids for increased electricity-assisted production of isobutanol by engineered *Shewanella oneidensis* MR-1. ACS Appl Mater Interfaces. 2017;9:43563–74.

Publisher's Note